

Band structure parameters of the nitrides: The origin of the small band gap of InN

Su-Huai Wei ^a, Pierre Carrier ^a

^a*National Renewable Energy Laboratory, Golden, Colorado 80401*

Abstract

Using a band-structure method that includes the correction to the band gap error in the local density approximation (LDA), we study the chemical trends of the band gap variation in III-V semiconductors and predict that the band gap for InN is 0.8 ± 0.1 eV, which is much smaller than previous experimental value of ~ 1.9 eV. The unusually small band gap for InN is explained in terms of the high electronegativity of nitrogen and consequently the small band gap deformation potential of InN. The possible origin of the measured large band gaps is discussed in terms of the non-parabolicity of the bands and the Moss-Burstein shift. Based on the error analysis of our LDA calculation and available experimental data we have compiled the recommended band structure parameters for wurtzite AlN, GaN and InN.

Key words: A1. Band structure parameters, B1. Nitrides, B2. Semiconducting III-V materials

PACS: 71.20.Nr, 71.15.Mb

Contacting information:

Dr. Su-Huai Wei
National Renewable Energy Laboratory
1617 Cole Blvd.
Golden, CO 80401, USA
Tel: (+1) 303-384-6666; Fax: (+1) 303-384-6432
email: swei@nrel.gov

1 Introduction

III-nitrides are usually considered as wide-band gap materials that have applications in devices such as ultraviolet/blue/green light-emitting diodes and lasers [1]. However, recent measurements suggest that the band gap of wurtzite (WZ) InN is below 1.0 eV [2,3,4,5,6], much smaller than the 1.89 eV band gap [7] widely accepted in the past to interpret experimental data [1] and to fit empirical pseudopotentials for modeling InN and related alloy properties [8,9]. If InN indeed has a less than 1.0 eV band gap, which is even smaller than that for InP (1.4 eV) [10], then InN and its III-nitride alloys could also be suitable for low band gap device applications such as future-generation solar cells because the nitride alloys can cover the whole solar spectrum range.

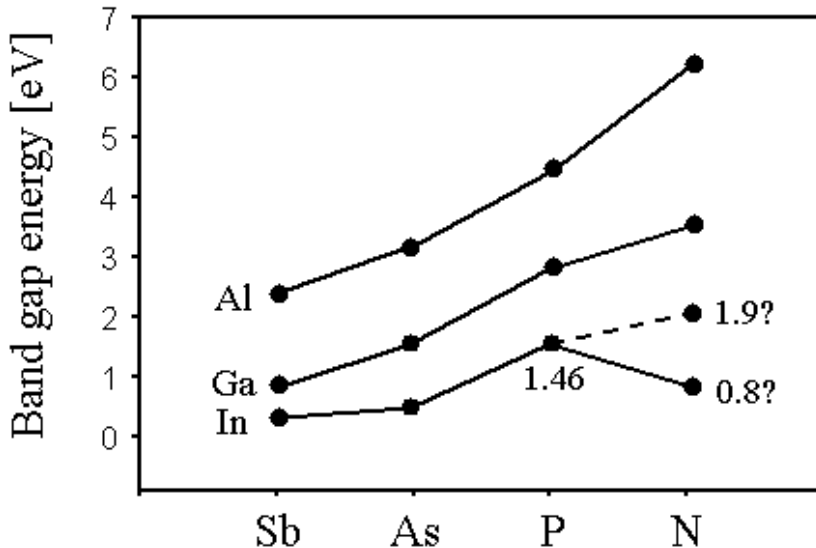


Fig. 1. Band gap as a function of anions for III-V semiconductors. See text for details.

The possible low band gap of InN also provides a challenge to understand the general chemical trends of semiconductor band gaps [11,12]. Conventional wisdom holds that for common-anion (or cation) III-V semiconductors, the direct band gap at Γ increases as the cation (or anion) atomic number decreases [the band gap-common-anion (or cation) rule]. This observation is strongly supported by experimental data [10] shown in Figure 1. For example, the direct band gaps of the common-anion compounds InAs, GaAs, and AlAs increase from 0.42 to 1.52 to 3.13 eV. Similarly, the direct band gaps of the common-cation zinc-blende (ZB) compounds GaSb, GaAs, GaP, and GaN increase from 0.81 to 1.52 to 2.86 to 3.32 eV. This trend also would hold for common-cation InX (X=N, P, As, Sb) compounds if $E_g(\text{InN}) = 1.9$ eV, as previously reported

Table 1

LDA calculated structural parameters of AlN, GaN, and InN. Results are compared with available experimental data (in parenthesis). ΔE_{ZB-WZ} is the calculated total energy difference between the ZB and WZ phases. Positive number indicate the WZ structure is more stable, in agreement with experiment.

| properties | AlN | GaN | InN |
|---------------------------------|---------------|---------------|---------------|
| a (Å) | 3.098 (3.112) | 3.170 (3.189) | 3.546 (3.544) |
| c/a (Å) | 1.601 (1.601) | 1.625 (1.626) | 1.612 (1.613) |
| u | 0.3819 | 0.3768 | 0.3790 |
| a_{ZB} (Å) | 4.355 (4.36) | 4.476 (4.50) | 4.964 (4.98) |
| ΔE_{ZB-WZ} (meV/2-atom) | 45 | 11 | 21 |

[7]. However, the rule will be broken if $E_g(\text{InN}) \sim 0.8$ eV as reported in recent measurements [2,3,4,5,6].

Direct theoretical calculation of the band gap of InN is not straightforward, mainly because in modern band structure calculations employing the local density approximation (LDA) [13], the calculated semiconductor band gap is severely underestimated [14,15]. For example, the LDA-calculated band gap of GaAs (~ 0.1 eV) is much smaller than the experimental value of 1.52 eV. For InN in the WZ structure, the LDA-calculated band gap is about -0.4 eV. This value is clearly much smaller than the true band gap of InN. Various approaches such as the GW and the self-interaction correction (SIC) methods have been tried in the past to correct the LDA band gap error [16,17,18,19]. Although there are strong indications from recent calculations [12,20] that the true band gap of InN should be much smaller than the previously reported experimental value of 1.9 eV, the uncertainty of these calculations is still quite large. Depending on the different treatments, the predicted band gap values for InN varies from 0.0 eV to 1.8 eV [16,17,18,19]. This is partly because the presence of the In $4d$ orbitals in the valence bands and partly because the LDA calculated band gap for InN is negative [20].

In this paper, to predict the InN band gap and understand the origin of the InN band gap anomaly, we have performed LDA-based band-structure calculations using a semiempirical method in which the LDA band gap error are corrected [12]. We find that the band gap of WZ InN is 0.8 ± 0.1 eV, in good agreement with recent experimental measurements. We show that the reason that InN has a smaller band gap than InP is due to the much large electronegativity and the much smaller band gap deformation potential for InN. The semiempirical approach is also applied to analyze the LDA error in the calculated band structure parameters. Based on this analysis, more realistic band structure parameters for the III-nitrides are recommended.

Table 2

Fitted parameters \bar{V} , V_0 , and r_0 for group III and group V atoms. ES denotes empty sphere. For nitrides, $R_{MT}(ES) = 1.68$ a.u.. For all other compounds, $R_{MT}(ES) = 2.05$ a.u..

| Atom | \bar{V} (Ry) | V_0 (Ry) | r_0 (a.u) |
|--------------|----------------|------------|-------------|
| N, P, As, Sb | 0.00 | 80 | 0.025 |
| Al | 0.00 | 360 | 0.025 |
| Ga | 0.00 | 280 | 0.025 |
| In | 0.00 | 200 | 0.025 |
| <i>ES</i> | 0.36 | 100 | 0.025 |

2 Method of calculations

The band structure calculations in this study are performed using the fully relativistic (including spin-orbit coupling), general potential, linearized augmented plane wave (LAPW) method [21]. Highly converged k-points sampling for the Brillouin zone integration and cut-off energy for the basis function are used. The Ga 3*d* and In 4*d* states are treated as valence electrons. The band structures are calculated at experimental lattice constants [10]. For the III-nitride compounds, the LDA calculated structural parameters (Table I) are in very good agreement with the available experimental data. The absorption coefficients for the nitrides are calculated using the optical package in WIEN2K [22].

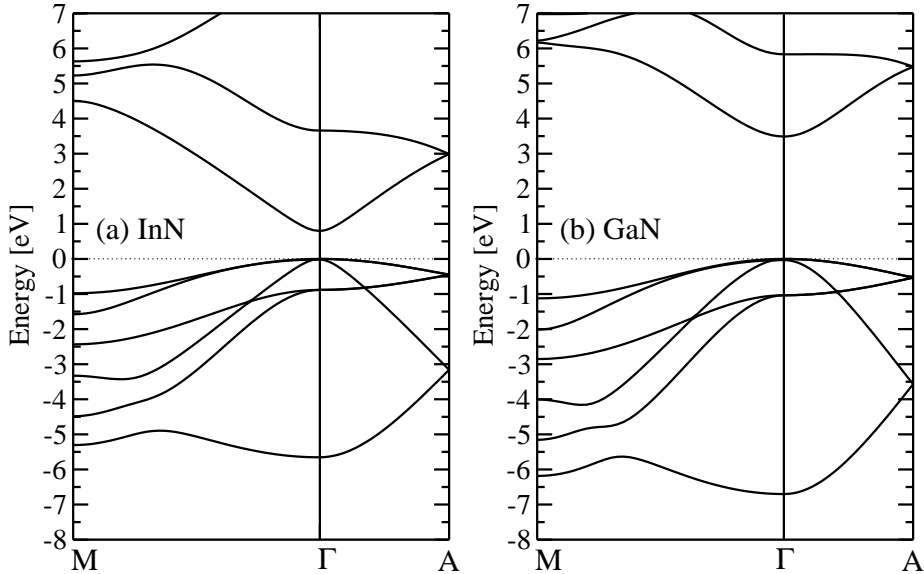


Fig. 2. Calculated band structure of (a) wurtzite InN and (b) wurtzite GaN. The energy zero is set at valence band maximum (VBM).

Although LDA is accurate in predicting the ground state properties such as

Table 3

Calculated band gaps at Γ for ZB and WZ III-V compounds at experimental (exp) lattice constants using the LDA-plus-correction (LDA+C) methods. The E_g^{LDA+C} values with an (*) are fitted values, whereas all the others are predicted values. Our calculated results are compared with available experimental data [10]. The last column show the error between predicted values and the experimental data.

| | a_{exp} (Å) | E_g^{LDA+C} (eV) | E_g^{exp} (eV) | $ \delta E_g $ (eV) |
|---------|---------------|--------------------|------------------|---------------------|
| AlSb | 6.133 | 2.28 | 2.32 | 0.04 |
| GaSb | 6.096 | 0.81 | 0.81 | 0.00 |
| InSb | 6.479 | 0.15 | 0.24 | 0.09 |
| AlAs | 5.660 | 3.05 | 3.13 | 0.08 |
| GaAs | 5.653 | 1.43 | 1.52 | 0.09 |
| InAs | 6.058 | 0.36 | 0.42 | 0.06 |
| AlP | 5.467 | 4.42* | 4.38 | 0.04 |
| GaP | 5.451 | 2.86* | 2.86 | 0.00 |
| InP | 5.869 | 1.40* | 1.46 | 0.06 |
| AlN | 4.360 | 6.00 | — | — |
| GaN | 4.500 | 3.34* | 3.32 | 0.02 |
| InN | 4.980 | 0.70 | — | — |
| | a=3.112 | | | |
| AlN(WZ) | c=4.982 | 5.95 | 6.1 | 0.15 |
| | u=0.3819 | | | |
| | a=3.189 | | | |
| GaN(WZ) | c=5.185 | 3.49 | 3.5 | 0.01 |
| | u=0.3768 | | | |
| | a=3.544 | | | |
| InN(WZ) | c=5.718 | 0.85 | — | — |
| | u=0.3790 | | | |

the lattice parameters, it is well known that it severely underestimates the semiconductor band gap [14]. To correct the LDA band gap error, we use a well established approach by adding to the LDA potential δ -function-like external potentials [23,24] inside the muffin-tin (MT) spheres centered at each atomic site α

$$V_{ext}^\alpha(r) = \bar{V}^\alpha + V_0^\alpha \left(\frac{r_0^\alpha}{r}\right) e^{-\left(\frac{r}{r_0^\alpha}\right)^2}, \quad (1)$$

Table 4

Calculated (LDA+C) direct band gaps (in eV) at Γ of zinc-blende Al, Ga, and In compounds at their equilibrium (eq) lattice constants and at their respective phosphides lattice constants.

| | $a = a_{\text{AlP}}$ | a_{eq} | | $a = a_{\text{GaP}}$ | a_{eq} | | $a = a_{\text{InP}}$ | a_{eq} |
|------|----------------------|----------|------|----------------------|----------|------|----------------------|----------|
| AlN | 0.45 | 6.00 | GaN | -0.61 | 3.34 | InN | -1.27 | 0.70 |
| AlP | 4.42 | 4.42 | GaP | 2.86 | 2.86 | InP | 1.40 | 1.40 |
| AlAs | 4.04 | 3.05 | GaAs | 2.36 | 1.43 | InAs | 0.92 | 0.36 |
| AlSb | 5.69 | 2.28 | GaSb | 3.67 | 0.81 | InSb | 2.15 | 0.15 |

and performed the calculation self-consistently. This functional form of the correction potential is based on the observation that the LDA band gap error is orbital dependent. To correct the band gap error, one needs to have a potential that is more repulsive to the s orbital than to the p orbital. Because the p orbital has zero charge density at the nuclear site, whereas the s orbital has finite density at the nuclear site, a δ -like potential centered at the nuclear site can increase the band gap. The parameters in Eq. (1) are fitted first only to the available experimental energy levels and to the quasiparticle energies [14] at *high-symmetry* k -points for AlP, GaP, InP, and GaN [24]. To improve the fit, empty spheres centered at tetrahedral sites are also used and a constant potential term $\bar{V}^\alpha = 0$ is added only at the empty sphere sites. The MT radii for the empty sphere are 2.05 a.u. except for zinc-blende (ZB) nitrides where we used $R_{MT} = 1.68$ a.u. to avoid having overlapping MT spheres. The fitting parameters are given in Table II. The *same parameters* given in Table II are then used to predict the band gaps of arsenides, antimonides, and nitrides. To find the band gap for the wurtzite structure, we add the LDA-calculated band gap differences between the WZ and ZB compounds to the calculated band gaps for the ZB compound. This is done to avoid using extra fitting parameters because a smaller empty sphere has to be used in the wurtzite structure.

Table 5

Calculated atomic s and p orbital energies for group III and group V elements.

| Atom | ϵ_s (eV) | ϵ_p (eV) |
|------|-------------------|-------------------|
| Al | -7.91 | -2.86 |
| Ga | -9.25 | -2.81 |
| In | -8.56 | -2.78 |
| N | -18.49 | -7.32 |
| P | -14.09 | -5.68 |
| As | -14.70 | -5.34 |
| Sb | -13.16 | -5.08 |

Comparing to our directly calculated results for the wurtzite structure, we find that this procedure is reliable. The overall uncertainty of the predicted band gap associated with this fitting procedure is estimated to be less than 0.1 eV. The effective mass are calculated using two definitions. For the density of state effective mass m_D that is related to Moss-Burstein shift [25], it is given by

$$m_D(\mathbf{k}) = \frac{\hbar^2 k^2}{2E(\mathbf{k})} . \quad (2)$$

For the wurtzite compounds with anisotropic band we define $m_D^* = [(m_D^\perp)^2 m_D^\parallel]^{1/3}$, where m_D^\perp and m_D^\parallel are the effective masses perpendicular and parallel to the c axis, respectively. For transport effective mass m_T , it can be calculated using the definition that

$$m_T = \frac{\hbar^2 k}{dE(\mathbf{k})/d\mathbf{k}} . \quad (3)$$

The two definitions are identical at Γ or if the band is parabolic, but could be significantly different at large \mathbf{k} when the band is non-parabolic. For most semiconductors $E(\mathbf{k})$ contains additional terms of the order k^4 [10], therefore, near the conduction band minimum (CBM) the electron effective mass increases linearly as a function of the band edge energy E and the slope of m_T versus E is about twice as larger as the slope of m_D versus E . It is well know that LDA also underestimate the calculated effective masses. Similar to the treatment for the band gap, we have fitted our results for GaN and GaAs, and applied the same procedures to calculate the effective masses for AlN and InN.

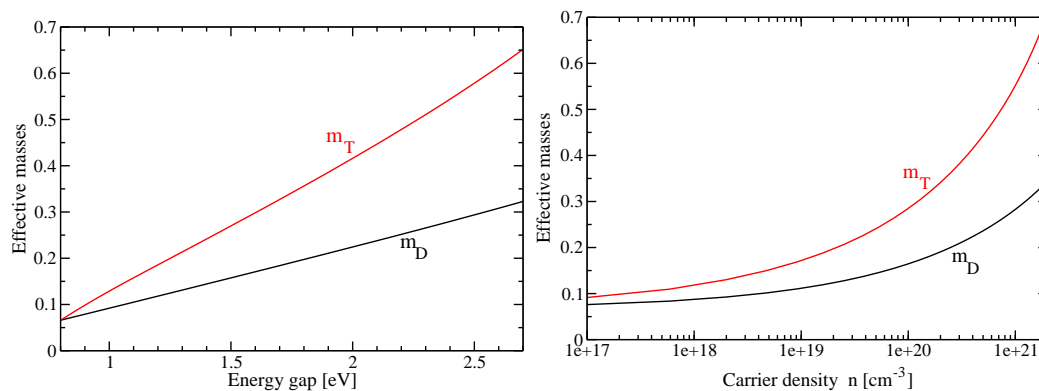


Fig. 3. Calculated electron effective masses as a function of (a) the absorption edge energy and (b) the carrier density. The definition of m_D and m_T are given in Eq. (2) and Eq. (3), respectively.

3 Results and discussions

3.1 Band gap of InN

The predicted direct band gaps at the Γ -point for the III-V semiconductors are shown in Table III. These values are compared with available experimental data [10]. We find that for nearly *all* the III-V semiconductors, the differences between the predicted and the experimental band gaps are less than 0.1 eV. For InN, however, our predicted value of 0.85 eV is much smaller than the previous experimental value [7] of 1.9 eV, but it is in very good agreement with recent experimental measurements [2,3,4,5,6]. For AlN, our predicted band gap of 6.0 eV is also close to recent photoluminescence measurement of 6.1 eV [26], which is smaller than previously accepted value around 6.3 eV [1,10,27].

3.2 Chemical trends of the band gap of III-V semiconductors

Our calculations above show convincingly that the band gap of InN is around 0.8 ± 0.1 eV. However, this value is about 0.6 eV smaller than that of InP, thus contradicting the conventional wisdom that the band gaps of common-cation (or anion) compounds increase as the anion (cation) atomic number decreases (Fig. 1). To understand the origin of the breakdown of the band gap common-cation rule in In compounds, we study the chemical and size contributions to the band gap in III-V semiconductors. For the chemical contribution, we calculate the band gaps of Al, Ga, and In compounds at the *fixed lattice constants* of AlP, GaP, and InP, respectively. The results are shown in Table IV. LDA corrections (LDA+C) are included. We find that at the phosphide volume, the band gaps of the common-cation system decrease from *MSb* to *MP* to *MAs* to *MN* (M =Al, Ga, and In), following the same trend of the anion atomic valence *s* orbital energies shown in Table V. This is because the conduction band minimum (CBM) at the Γ -point is an anion *s* plus cation *s* state. The anion contribution increases as the compound becomes more ionic. Because the N 2*s* orbital energy is much lower in energy than the Sb 5*s*, As 4*s* and P 3*s* orbital energies (Table V), respectively, the band gap of the nitrides are also much lower than the corresponding antimonides, arsenides, and phosphides at fixed volume.

Because the order of the band gaps calculated at the fixed volume is generally opposite to what is observed at the equilibrium lattice constants, the chemical contribution alone cannot explain the experimentally observed trend in the band gaps at equilibrium lattice constants. Next, we investigate the size

Table 6

Calculated band gap volume deformation potential $a_g = dE_g/d\ln V$ at Γ for III-V semiconductors.

| Compound | $-a_g$ | Compound | $-a_g$ | Compound | $-a_g$ |
|--------------|------------|--------------|----------|--------------|----------|
| AlN (ZB; WZ) | 10.2; 10.4 | GaN (ZB; WZ) | 7.4; 7.8 | InN (ZB; WZ) | 3.7; 4.2 |
| AlP | 9.5 | GaP | 8.8 | InP | 5.9 |
| AlAs | 8.9 | GaAs | 8.2 | InAs | 5.7 |
| AlSb | 8.9 | GaSb | 8.0 | InSb | 6.4 |

or volume deformation contribution to the band gap. The calculated volume deformation potentials [28] $a_g = dE_g/d\ln V$ with the LDA correction for III-V semiconductors are listed in Table VI. We see that all the compounds have negative volume deformation potentials at Γ , i.e., when the volume decreases, the band gap increases. Therefore, it is clear that the observed common-cation rule and the common-anion rule for the band gap is mainly due to the large deformation potential of the III-V compounds. For example, at GaP lattice constant, the band gap of GaSb is 0.81 eV larger than that of GaP. However, GaSb is about 34% larger in volume than GaP. So, with an average deformation potential of -8.4 eV, the band gap of GaSb at its equilibrium lattice constant is about 2.05 eV smaller than the band gap of GaP at its equilibrium lattice constant. The same situation also applies to AlN and GaN versus AlP and GaP, respectively, because AlN and GaN have large band gap deformation potentials [$a_g(\text{AlN}) = -10.4$ eV and $a_g(\text{GaN}) = -7.8$ eV]. However, for InN, although its volume is about 49% smaller than InP, its band gap deformation potential is small, $a_g(\text{InN}) = -4.2$ eV. Because of this small $|a_g|$, the contribution due to the size or deformation potential (~ 2.1 eV) is not sufficient to reverse the order of the band gap due to the contribution of the chemical effect (~ -2.7 eV). This explains why InN has a band gap about 0.6 eV smaller than that of InP.

From the analysis above, we see that the breakdown of the common-cation rule for the band gap in In compounds is due to the small $|a_g|$. We find that [28], the small $|a_g|$ for InN is due to the combined effects of (i) a large difference between the cation In 5s and anion N 2s orbital energies, (ii) a large repulsion between the N 2p and the high-lying In 4d orbitals, and (iii) a large In-N bond length (relative to AlN and GaN). Because a similar situation also exists in II-VI semiconductors, one would expect that the breakdown of the common-cation rule should also apply to the II-VI systems. Indeed, experimental data [10] show that the ZnO band gap of 3.4 eV is smaller than the ZnS band gap of 3.8 eV. Our calculations also show that CdO and HgO would have band gaps that are about 0.5 eV smaller than the band gaps of CdS and HgS, respectively, if they could all exist in the ZB phase.

Table 7

Recommended band structure parameters at Γ for unstrained AlN, GaN, and InN. The properties show in this table are the band gap E_g , the spin-orbit splitting Δ_0 , the crystal field splitting Δ_{CF} , the valence band splittings ΔE_{12} and ΔE_{13} , and the effective masses m parallel and perpendicular to the c axis. The averaged effective mass can be obtained using $m^* = [(m^\perp)^2 m^\parallel]^{1/3}$.

| Properties | AlN | | GaN | | InN | | |
|-----------------------|---------|-------------|------------------|-------------|---------|-------------|--|
| $E_g(\text{WZ})$ (eV) | 6.10 | | 3.51 | | 0.78 | | |
| $E_g(\text{ZB})$ (eV) | 6.15 | | 3.35 | | 0.70 | | |
| Δ_0 (meV) | 19 | | 16 | | 5 | | |
| Δ_{CF} (meV) | -224 | | 25 | | 19 | | |
| ΔE_{12} (meV) | 218 | | 8 | | 3 | | |
| ΔE_{13} (meV) | 237 | | 33 | | 21 | | |
| | | | effective masses | | | | |
| | \perp | \parallel | \perp | \parallel | \perp | \parallel | |
| $m_A(m_0)$ | 4.35 | 0.28 | 0.39 | 2.04 | 0.14 | 2.09 | |
| $m_B(m_0)$ | 0.67 | 3.50 | 0.43 | 0.85 | 0.13 | 0.50 | |
| $m_C(m_0)$ | 0.68 | 3.43 | 1.05 | 0.19 | 0.81 | 0.07 | |
| $m_e(m_0)$ | 0.33 | 0.32 | 0.22 | 0.20 | 0.07 | 0.06 | |

3.3 Possible origin of the measured large band gap for InN

Our calculation and analysis above show that the fundamental band gap of InN is indeed small, around 0.8 eV. To understand the origin of some of the experiments which show large band gap of InN [7,29,30], we have performed detailed study of the band structure of InN. Experimentally, one often assumes that the band edge states near Γ is parabolic and the dipole transition matrix element is nearly independent of \mathbf{k} , therefore, the absorption coefficient squared α^2 is a linear function of the absorption energy E . The fundamental band gap, thus, can be obtained from the interception with the energy axis by drawing a straight line in the α^2 versus E plot [7,29,30]. To test the validity of this assumption, we show in Figure 2 the calculated band structure of wurtzite InN. Figure 3 shows the calculated electron effective masses, and Figure 4 shows our calculated absorption coefficients of InN. For comparison, we also calculate the band structure and absorption coefficients of GaN. We find that the conduction band of InN is strongly non-parabolic (Fig.2). This is confirmed from the calculated electron effective masses (Fig. 3), which increase significantly with the band edge energy or electron concentration. If the conduction band was parabolic the electron effective mass would be a constant.

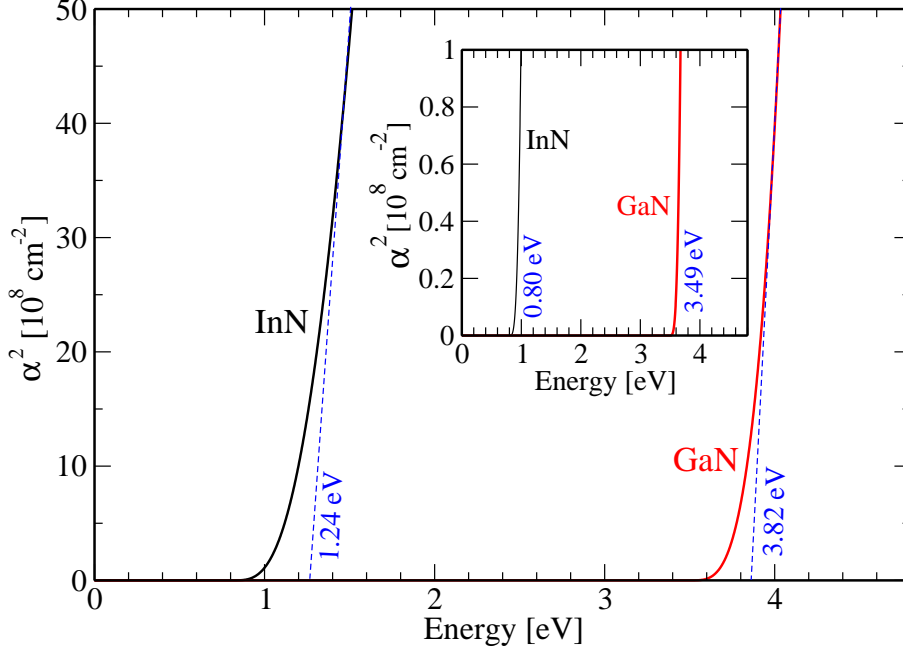


Fig. 4. Calculated absorption coefficients of InN and GaN. We show that using the linear extrapolation technique the apparent measured band gaps depend on the scale used in the extrapolation.

Because of the large deviation from the parabolic band, the calculated α^2 is not a linear function of E (Fig. 4). Therefore, if one use the linear extrapolation technique to determine the band gap, the derived apparent band gaps depend on where the straight lines are drawn. For example, as shown in Fig. 4 for InN, using large values of the absorption coefficient to draw the straight line, one can obtain an apparent band gap that is about 0.4 eV larger than the fundamental band gap. The dependence is relatively smaller for GaN which has a larger effective mass than that of InN, thus a larger density of states near the CBM and a sharper increase of the absorption coefficient. We notice that the samples used to obtain the large InN band gaps [7,29,30] often have poor sample quality and the band gaps are usually estimated from the absorption spectra with large absorption coefficients. We also notice that the InN samples that show large band gaps often have high oxygen concentration [29] and are heavily n-type doped [7,29,30]. Besides the possible formation of InNO alloys as proposed in Ref. [29], this observation suggests that the measured absorption edge can be shifted by the Moss-Burstein effect [25]. Figure 5 shows our calculated absorption edge energy as a function of the carrier density. We see that the absorption edge increases with the carrier density from 0.8 eV for intrinsic InN to ~ 2.5 eV for sample with electron concentration of $\sim 10^{21}$ cm $^{-3}$. These results are consistent with recent experimental observation [31].

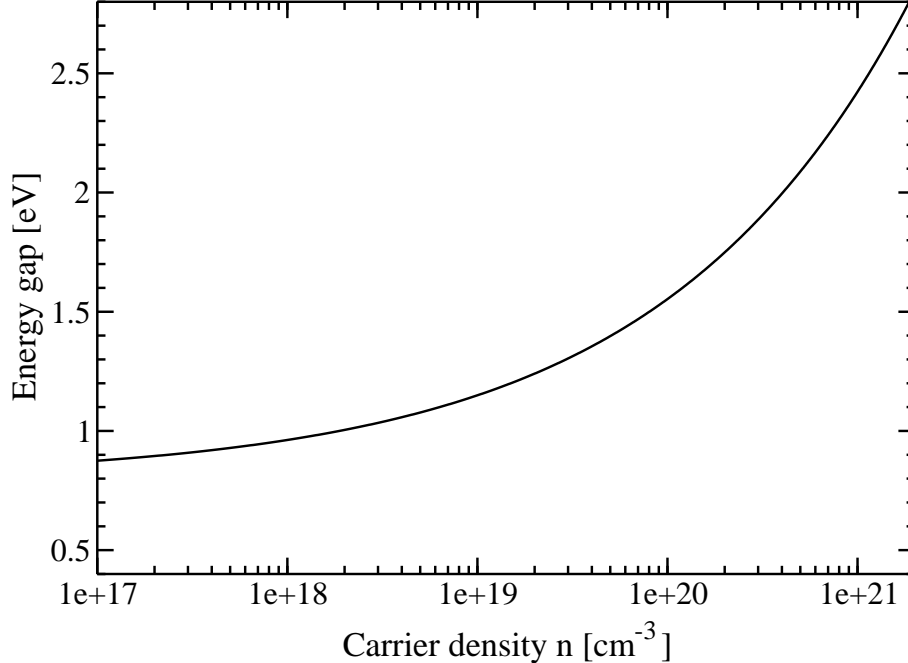


Fig. 5. Calculated Moss-Burstein shift of the absorption edge energy as a function of the carrier density.

4 Band structure parameters of nitrides

In the last few years several excellent review articles [32,33] and books [1,27] have been published to describe the band structure parameters of InN and other III-nitride. The recommended band structure parameters are based on a collection of available experimental data and theoretical calculations. The approach used in this study enabled us to analyze the degree of the systematic LDA errors on the band structure parameters of the III-nitrides. For example, we find that the LDA not only underestimates the band gap, but it also slightly underestimated the crystal field splittings Δ_{CF} and the spin-orbit splittings Δ_0 at the top of the valence band, as well as the electron and light hole effective masses. Details of the analysis will be published elsewhere. Based on the LDA error analysis and comparison with available experimental data we propose here the recommended band structure parameters for the III-nitrides shown in Table VII. We suggest that these parameters should be used in the future to fit empirical pseudopotentials to study the nitride systems.

5 Summary

In summary, using an empirical LDA-based band structure method with band gap correction we have systematically studied the chemical trends of the band

gap variation in III-V semiconductors. We find that InN has a band gap of 0.8 ± 0.1 eV, in good agreement with recent experimental measurements. We show that the previously accepted band gap-common-cation rule does not hold for ionic InN and the II-VI oxides. We have also compiled the recommended band structure parameters for AlN, GaN, and InN.

6 Acknowledgment

We would like to thank I. G. Batyrev, X. Nie, S. B. Zhang, S. R. Kurtz, H. X. Jiang, Y. F. Chen, and G. X. Gao for many valuable discussions. This work is supported by the U.S. Department of Energy, Contract No. DE-AC36-99GO10337.

References

- [1] H. Morkoç, *Nitride Semiconductors and Devices*, (Springer, New York, 1999).
- [2] T. Inushima, V. V. Mamutin, V. A. Vekshin, S. V. Ivanov, T. Sakon, M. Motokawa, and S. Ohoya, *J. Crystal Growth* 227/228 (2001) 481.
- [3] V. Yu Davydov et al., *Phys. Stat. Sol. (b)* 230 (2002) R4; *Phys. Stat. Sol. (b)* 229 (2002) R1; *Phys. Stat. Sol. (b)* 234 (2002) 787.
- [4] J. Wu, W. Walukiewicz, K. M. Yu, J. W. Ager III, E. E. Haller, H. Lu, J. Schaff, Y. Saito, and Y. Nanishi, *Appl. Phys. Lett.* 80 (2002) 3967.
- [5] J. Wu, W. Walukiewicz, K. M. Yu, J. W. Ager III, E. E. Haller, H. Lu, J. Schaff, *Appl. Phys. Lett.* 80 (2002) 4741.
- [6] A. Yamamoto, K. Sugita, H. Takatsuka, A. Hashimoto, V. Yu. Davydov, *J. Crystal Growth* 261 (2004) 275.
- [7] T. L. Tansley and C. P. Foley, *J. Appl. Phys.* 59 (1986) 3241.
- [8] L. Bellaiche, T. Mattila, L. W. Wang, S.-H. Wei, and A. Zunger, *Appl. Phys. Lett.* 74 (1999) 1842.
- [9] P. R. C. Kent and A. Zunger, *Appl. Phys. Lett.* 79 (2001) 1977.
- [10] *Intrinsic Properties of Group IV Elements and III-V, II-VI, and I-VII compounds*, edited by O. Madelung, M. Schulz, and H. Weiss, Landolt-Bornstein, New Series, Group III, Vol. 22, Pt. a (Springer, Berlin, 1987).
- [11] B. R. Nag, *Phys. Stat. Sol. (b)* 233, (2002) R8.
- [12] S.-H. Wei, X. Nie, I. G. Batyrev, and S. B. Zhang, *Phys. Rev. B* 67, (2003) 165209.

- [13] P. Hohenberg and W. Kohn, Phys. Rev. 136 (1964) B864; W. Kohn and L. J. Sham, *ibid.* 140, (1965) A1133.
- [14] X. Zhu and S. G. Louie, Phys. Rev. B 43 (1991) 14142.
- [15] A. Rubio, J. L. Corkill, M. L. Cohen, E. L. Shirley, and S. G. Louie, Phys. Rev. B 48 (1993) 11810.
- [16] M. van Schilfgaarde, A. Sher, A.-B. Chen, J. Cryst. Growth 178 (1997) 8; A. Sher, M. van Schilfgaarde, M. A. Berding, S. Krishnamurthy, and A.-B. Chen, MRS Internet J. Nitride Semicon. Res. 4S1, (1999) G5.1. 5A
- [17] T. Kotani and M. van Schilfgaarde, Solid State Commun. 121 (2002) 461.
- [18] D. Vogel, P. Kruger, and J. Pollmann, Phys. Rev. B 55 (1997) 12836; C. Stampfl, C. G. Van de Walle, D. Vogel, P. Kruger, and J. Pollmann, Phys. Rev. B 61 (2000) R7846.
- [19] K. A. Johnson and N. W. Ashcroft, Phys. Rev. B 58 (1998) 15548.
- [20] F. Bechstedt and J. Furthmuller, J. Crystal Growth 246 (2002) 315.
- [21] S.-H. Wei and H. Krakauer, Phys. Rev. Lett. 55 (1985) 1200; D. J. Singh, *Planewaves, Pseudopotentials, and the LAPW Method*, (Kluwer, Boston, 1994).
- [22] P. Blaha, K. Schwarz, G. K. H. Madsen, D. Kvasnicka, and J. Luitz, WIEN2k code, Vienna University of Technology, November 2001; P. Blaha, K. Schwarz, P. Sorantin, and S. B. Trickey, Comput. Phys. Commun. 59 (1990) 399.
- [23] N. E. Christensen, Phys. Rev. B 30 (1984) 5753.
- [24] S. H. Wei and A. Zunger, Phys. Rev. B 57 (1998) 8983.
- [25] T. S. Moss, Proc. Phys. Soc. London B 67 (1954) 775; E. Burstein, Phys. Rev. 93 (1954) 632.
- [26] J. Li, K. B. Nam, M. L. Nakarmi, J. Y. Lin, H. X. Jiang, P. Carrier, and S.-H. Wei, Appl. Phys. Lett. 83 (2003) 5163.
- [27] *Properties of Group III Nitrides*, edited by J. H. Edgar, (INSPEC, London, 1994).
- [28] S.-H. Wei and A. Zunger, Phys. Rev. B 60 (1999) 5404.
- [29] Motlan, E. M. Goldys, and T. L. Tansley, J. Crystal Growth 241, (2002) 165.
- [30] K. Osamura, K. Nakajima, Y. Murakami, P. H. Shingu, and A. Ohtsuki, Solid State Commun. 11 (1972) 617; K. Osamura, S. Naka, Y. Murakami, J. Appl. Phys. 46 (1975) 3432.
- [31] J. Wu, W. Walukiewicz, W. Shan, K. M. Yu, J. W. Ager III, E. E. Haller, H. Lu, W. J. Schaff, Phys. Rev. B 66 (2002) 201403.
- [32] I. Vurgaftman and J. R. Meyer, J. Appl. Phys. 94 (2003) 3675.
- [33] A. G. Ghuiyan, A. Hashimoto, and A. Yamamoto, J. Appl. Phys. 94 (2003) 2779.